Thymus formation in uncharted embryonic territories.

Isabel Alcobia[a,b,*], Margarida Gama-Carvalho[c,*], Leonor Magalhães[a,*], Vitor Proa[a] , Domingos Henrique[a,b], Hélia Neves[a,b,**]

[a]Universidade de Lisboa, Faculdade de Medicina, Instituto de Histologia e Biologia do Desenvolvimento, Lisboa, Portugal;

[b] Universidade de Lisboa, Instituto de Medicina Molecular, Lisboa, Portugal.

[c] BioISI – Biosystems & Integrative Sciences Institute, Faculty of Sciences, University of Lisboa, 1749-016, Lis-boa, Portugal.

Isabel Alcobia: halcobia@medicina.ulisboa.pt; halcobia@campus.ul.pt

Margarida Gama-Carvalho: mhcarvalho@fc.ul.pt

Leonor Magalhães: leonorhelena@campus.ul.pt

Vitor Proa: vitorproa@medicina.ulisboa.pt

Domingos Henrique: henrique@medicina.ulisboa.pt

Hélia Neves: helia.neves@campus.ul.pt; hneves@medicina.ulisboa.pt

*First co-authors

**Author for correspondence: helia.neves@campus.ul.pt; hneves@medicina.ulisboa.pt

Phone +351 21 7999528

Fax +351 21 7999527

Keywords: Thymic molecular signature; local mesenchymal modulators; high-throughput sequencing data.

ABSTRACT

The thymus is a conserved organ among vertebrates, derived from the endoderm of distinct pharyngeal pouches (PP), whose location and number vary in different species. Together with reports of sporadic ectopic thymus locations in mice and humans, this suggests that the potential to make a thymus resides in a broader region of the PP endoderm than previously ascribed.

Using the chick-quail chimera system, we explore this hypothesis and test the capacity of non-canonical pouches to participate in thymus formation. We further ask if the local mesenchyme of pharyngeal arches (PA) could also play a role in the regulation of thymus formation.

After testing several embryonic tissue associations, we mapped the pharyngeal endoderm regions with thymus potential to the second and third/fourth pharyngeal pouches (2PP and 3/4PP). We further identified mesenchyme regions that regulate this potential to the the 3/4 pharyngeal arches and to the dorsal region of the second arch, with positive and negative influences, respectively.

Transcriptomic analysis of these tissues helped us to delineate a common genetic program correlated with thymus potential in the endoderm, and to define distinct signalling pathways acting in mesenchymal environments to help patterning pharyngeal arches. Together, these results provide new information about the initial specification of thymus primordia in the embryo and might help in improving thymus organoid systems.

INTRODUCTION

The thymus is a primary lymphoid organ essential for T lymphocyte development and maturation. The generation of a self-tolerant and diverse repertoire of T cell receptors will ensure an effective recognition and abolition of foreign antigens in the periphery without mounting a deleterious immune response to the body's own tissues. This central immune tolerance is established by cellular interactions between differentiating lymphoid T-cells and a stromal microenvironment mainly formed by the thymic epithelium (TE) (Hamazaki, 2015; Duah M, 2021).

TE rudiment derives from the endoderm of the third and fourth pharyngeal pouches (3/4PP) as first demonstrated in 1975 using the chick-quail chimera system (Le Douarin and Jotereau, 1975).

Major efforts have been made to unveil the transcription factors and signalling molecules that play a role in the specification of the pharyngeal endoderm to thymus fate. Though Fork-head Box N1 (Foxn1) transcription factor appears as the earliest TE marker (Nehls et al., 1994) it is dispensable for its specification being needed only for TE maintenance and differentiation (Blackburn et al., 1996; Nehls et al., 1996). Other involved transcription factors are Pax1, Pax9, Hoxa3, Eya1, and Six1, whose abnormalities lead to impaired thymus organogenesis (Vaidya HJ et al., 2016). Recent studies integrating single-cell transcriptomes and chromatin accessibility analysis of the developing pharyngeal endoderm provided new insight into the progression from embryonic endoderm cells to the foetal thymus and the associated gene expression changes. Namely, Grhl3 was found to be a putative new transcriptional regulator of the medullary thymic epithelial sub-lineage (Park et al., 2020; Magaletta ME et al., 2022). In addition to the transcriptional factors portrayed signalling pathways like bone morphogenetic protein (BMP), fibroblast growth factor (FGF), Wingless-int (Wnt), Notch, and Hedgehog, were also shown to be involved in the 3/4PP patterning and the early phases of thymus organogenesis (reviewed in Figueiredo M et al., 2020). We have previously described the requirement of Notch signalling for TE specification and parathyroid epithelium differentiation, in a manner that is Hedgehog dependent (Figueiredo et al., 2016). In addition, Foxn1 expression was unexpectedly detected in the 2PP, and its expression modulated by Hedgehog signalling, identical to what occurs at 3/4PP (Figueiredo et al., 2016). These findings suggest that Foxn1-expression domains in the distinct endodermal pouches may embody a conserved potential to develop a thymus. In agreement, the thymus derives from different pouches among jawed vertebrates (Rodewald, 2008), and accessory thymi can be found in the cervical region in humans (Norris, 1938; Van Dyke, 1941) and mice (Dooley et al., 2006; Terszowski, 2006).

Considering the known diversity of PP location of the thymic rudiment among vertebrates, we may envisage the existence of a phylogenetically conserved genetic program to "make a thymus" embodied in the endoderm of different PP, independent of their specific anatomical location. This program may be (or not) restricted by differential, yet unknown, molecular cues provided by the adjacent pharyngeal arch (PA) mesenchyme. To test this hypothesis, we took advantage of the modified chick-quail chimera system previously used (Figueiredo and Neves, 2018; Figueiredo and Neves, 2019; Figueiredo et al., 2016). We performed combinatorial heterospecific associations of pharyngeal pouches endoderm with

mesenchyme tissues from several embryonic locations and evaluated the potential to form a functional thymus. Additionally, genome-wide gene expression analysis by RNA-sequencing (RNA-seq) were performed in the different isolated regions of endoderm and mesenchyme. Our results show that non-canonical pharyngeal pouches can generate a morphological and functional thymus upon interactions with permissive mesenchyme. This indicates the existence of a conserved program embodied in the endoderm of different PP, independent of their specific anatomical location. Furthermore, we identify the dorsal region of the 2PA mesenchyme as having inhibitory properties to thymus formation. Transcriptomic analysis revealed a previously unnoticed Hox-code in the prospective thymus rudiment and specific signalling pathways activities according to the distinct mesenchymal environments of pharyngeal arches.

RESULTS AND DISCUSSION

The endoderm of the 2PP has similar thymic potential to the 3/4PP endoderm

During chicken embryonic development, thymic epithelium (TE) derives from the 3/4PP endoderm (canonical pouch). To evaluate the capacity of non-canonical pouches to form a thymus, we started by removing them from their natural environment and associate them with a permissive mesenchyme, the somatopleura mesoderm (SM). The SM capacity to support thymus development at ectopic locations in the embryo was previously demonstrated when grafting 3/4PP endoderm into the body wall of a chicken embryo (Le Lièvre and Le Douarin, 1975; Neves et al., 2012). Using a modified chick-quail chimera system, 2PP endoderm was isolated from quail (q) embryos at embryonic day 3 (E3) and *in vitro* associated with chicken (c) E2,5 somatopleura mesoderm, for 48h (Figueiredo and Neves, 2019; Neves et al., 2012). To evaluate the capacity of this heterospecific association to form a thymus, the 48h-cultured tissues were then grafted into the chorioallantoic membrane (CAM) of a chicken embryo (E8) and allowed to develop *in ovo* for further 10 days (Figueiredo and Neves, 2018; Figueiredo et al., 2016). The CAM behaves as a vascular supplier of nutrients and allows gas exchanges to grafted tissues, enabling their development *in ovo* for longer periods of time. In parallel, associations of 3/4PP endoderm (qE3) with SM (cE2,5) were used as positive control. Morphological analysis of tissues formed in CAM-explants was performed by conventional histology and immunohistochemistry, as previously described (Figueiredo and Neves, 2018; Figueiredo et al., 2016). Endoderm-derived cells were identified by immunohistochemistry using quail-specific antibody, mAb Quail PeriNuclear (QCPN).

Similar to control associations of 3/4PP endoderm, the 2PP endoderm-derived CAM-explants contained fully formed chimeric thymus with cortical and medullary compartments (Figure 1a

and Figure 1d). Quail-derived thymic epithelium displayed a reticular architecture (QCPN+, Figure 1b and Figure 1e) and it was colonized by lymphoid progenitor cells of donor origin (chicken) (Figure 1c and Figure 1f). The presence of CD3+ T-lymphocytes was also confirmed in these ectopic thymic structures. Considering pairwise developmental stage (qE12 and cE15), one in four lymphoid cells of chimeric thymus should express the CD3 marker (Ainsworth et al., 2010); and Figure S1 and Table S1). Similar CD3+ cell numbers were observed in chimeric thymus from 2PP or 3/4PP endoderm-derived CAM-explants (Figure 1c and Figure 1f).

The 2PP endoderm-derived CAM-explants with a fully formed thymus (n=6/6) were identical to those obtained when canonical 3/4PP was tested under the same conditions (n=5/5) (Table 1). These results point to the existence of a conserved program to form a thymus embodied in the endoderm of different PPs, independently of their specific anatomical location. Still, no thymus was formed when 1PP endoderm was associated with SM (n=5/6). Only small epithelial clusters were observed, with scarce CD3+ cells, suggesting a residual potential of this pouch endoderm to develop a thymic-like epithelium (Figure S2).

Remarkably, the 2PP endoderm-derived explants also gave rise to parathyroid glands (n=4/6; Table S2), suggesting an extended conservation mechanism in the formation of both organs, within distinct pouches.

The 2PP and 3PP endoderm share a conserved genetic program

Considering the capacity of 2PP endoderm to give rise to thymus epithelium, we then asked if this endoderm tissue could share a common genetic program with the 3/4PP endoderm. To evaluate this, the anterior endoderm region at qE3 was isolated (Figueiredo and Neves, 2019; Neves et al., 2012) and separated in three regions (Figure 2a): 2PP, 3/4PP and the central territory of anterior endoderm (pharynx), the latter as a negative control to thymic potential. Total RNA was isolated from three biological replicate samples of each region and used to generate libraries for Illumina paired-end mRNA-seq. High quality sequencing datasets were obtained for all samples, with an average 7 million reads mapping uniquely to the quail genome, corresponding to the detection of ~14 500 genes (Supplementary Dataset 1). Analysis of this dataset identified the differentially expressed (DE) genes between the three tissues (Figure 2b). Comparing the pouches' endoderm to pharynx, 555 and 492 up-regulated transcripts (log2FC >0.6, adj pval <0.01) were detected in 2PP and 3/4PP endoderm, respectively (Figure 2c and Figure 2d; the complete list of DE genes can be found in Supplementary Dataset 2). Of these, 262 transcripts were commonly up-regulated in both 2PP and 3/4 PP pouches, with 31 of these genes annotated as encoding Transcription Factors and Regulators (TF&R) (Figure 2c-2e).

A closer examination uncovered 31 up-regulated transcripts encoding Transcription Factors and Regulators (TF&R) common to PP endoderm (Figure 2e).

Considering the ability shown by the 2PP endoderm to mimic 3/4PP endoderm developmental potential, the set of commonly enriched transcripts should reflect a shared genetic program regulating the establishment of a general PP endoderm progenitor population (Figure 2e). One may wonder if a conserved thymic potential is embodied within this genetic program. In effect, various of these up-regulated transcripts encodes TF&Rs that have been shown to play crucial roles in early stages of T/PT organogenesis in mouse, chicken and human, namely EYA1/SIX1 (Li et al., 2003), NOTCH1/GLI3 (Figueiredo et al., 2016) and more recently NEUROD1 (Bautista et al., 2021; Park et al., 2020).

In addition, we found 3 transcripts encoding other TF&Rs, MEOX1, MAFB and FOXI2, which show higher expression in 3/4PP endoderm when compared to 2PP endoderm, suggesting the existence of an "intermediate" stage of commitment into 3/4PP endoderm, starting from the common progenitor. MABF and MEOX1 were mainly identified in parathyroid development (Kamitani-Kawamoto et al., 2011; Magaletta et al., 2022), while FOXI2 was shown to be expressed in PA mesenchyme of chicken embryos (Khatri and Groves, 2013). Conversely, we found 6 transcripts encoding TF&Rs with higher expression in 2PP endoderm (DLX3, EMX2, MSX1, TFAP2A, VGLL and TLX1), which might pinpoint to a similar "intermediate" stage of commitment into 2PP endoderm. Interestingly, TFAP2A acts up-stream of MSX1 and MAFB in neural crest progenitors (Enkhmandakh and Bayarsaihan, 2015), and mutations in this gene cause branchio-oculo-facial syndrome.

Lastly, our data also revealed the existence of a set of 23 transcripts encoding TF&Rs up-regulated in 2PP versus 3/4PP endoderm, and 33 TF&Rs upregulated in 3/4PP versus 2PP (Figure 2e and Figure S3). These two gene-sets may represent a further step into the gene cascade that regulates the acquisition of 2PP and 3/4PP identities.

Several up-regulated transcripts in 3/4PP endoderm encode TF&Rs like GCM2, HOXA3, GATA3, PAX1 and PAX9, which are known to be involved in 3/4PP patterning and T/PT common primordium specification in various animal models [reviewed in (Figueiredo et al., 2020)]. Others transcripts, encoding TF&Rs HOXA2, NKX2-5, MYC, GBX2, SALL1 and PRDM1, were recently detected in immature pharyngeal cells and thymic epithelium progenitors (Magaletta et al., 2022). We note a strong enrichment of transcripts encoding Hox genes in the 3/4PP endoderm, when compared to 2PP endoderm (Figure 3). This observation suggests the existence of a specific boundary in Hox gene expression at the interface between the second and third/fourth pharyngeal arches, likely important to define the identity of each pouch. Finally, we detected

up-regulation of two Notch-targets transcripts in 3/4PP endoderm, HEYL and HES5, pointing to an overlooked involvement of Notch activity in these early stages of thymus organogenesis.

The genetic signature of prospective thymic rudiment in 3/4PP endoderm.

While the previous analysis focused on examining gene expression changes that might underlie the initial acquisition of a thymic potential in the PP endoderm, understanding how thymus development is restricted to the 3/4PP endoderm might be better approached by directly comparing the transcriptomes of the 2PP and 3/4PP endoderm. This analysis revealed that 165 transcripts are upregulated in 3/4PP endoderm when comparing with 2PP endoderm, whereas 353 transcripts are downregulated (Figure 3a, and Supplementary Dataset 2).

inBio Discover analysis of these differentially expressed genes revealed GO-term enrichment mainly in morphogenesis and vascular development (Figure 3b). This analysis also revealed an association of 2PP endoderm up-regulated genes with GO-terms of negative regulation of developmental processes (Figure 3b).

Functional gene annotation identified 34 transcripts encoding TF&Rs specifically up-regulated in 3/4PP endoderm. 10 of these encode HOX TFs (Figure 3c and Figure 3d), and this strong enrichment in Hox gene expression in 3/4PP endoderm re-inforces the hypothesis that there is a clear identity boundary between 2PP and 3/4PP, probably critical for correct thymus specification. Indeed, HOXA2 and HOXA3 have been associated to T/PT formation, and HOXB1, HOXB2, HOXB4 and HOXB5 were recently associated to ultimobranchial body formation in mouse 4PP endoderm (Magaletta et al., 2022).

Of the remaining up-regulated TF&Rs in 3/4PP endoderm, SOX3 was shown to be required for PP formation and consequently to craniofacial morphogenesis (Rizzoti and Lovell-Badge, 2007). The analysis of TF&R genes in 2PP endoderm revealed a set of 40 up-regulated transcripts (Figure 3c and Figure 3d). Of these, GRHL3, TP63, TFAP2A, MSX1, MSX2, TBX10, DLX5 and SOX9 are known to be involved in orofacial cleft disease(Reynolds et al., 2019; Reynolds et al., 2020).

The mesenchyme of the PA modulates thymic potential of PP endoderm.

The capacity of 2PP endoderm to form a thymus when associated with ectopic mesenchyme reveals not only the thymic potential in this region but also that signals from adjacent PA mesenchyme are important to regulate such potential in PP endoderm. The fact that 2PP does not normally give rise to thymus might indicate that the underlying 2PA mesenchyme is unable to promote thymus development, or that it can even provide a local repressive environment for

thymus formation. Conversely, the mesenchyme of 3/4 PA is expected to produce signals that promote thymus formation in the overlying endoderm.

To test these hypotheses, 2PP endoderm was isolated from chicken embryos and associated *in vitro* with 3/4 PA mesenchyme, followed by growth *in ovo*, as described above. As expected, thymus was formed in 2PP endoderm-derived CAM-explants (n=3/3) with the typical thymic characteristics (Figures 4a-c). Similarly, thymus was formed in 3/4 PP and 3/4PA associations (n=3/3, Figures 4d-f). These results confirm the capacity of 3/4PA mesenchyme to promote thymus development.

To test for the presence of thymus-repressive signals in 2PA mesenchyme, its was associated with 3/4PP endoderm. Surprisingly, normal thymus was formed in CAM-explants derived from these associations (n=3/3, Figures 4g-i). Considering that thymic rudiments in chicken embryos emerge at the dorsal domain of 3/4PP, we asked whether the mesenchyme of the arches could have regionalized properties along the dorso-ventral axis. The 2PA mesenchyme was isolated and further sectioned into dorsal (2PAd) and ventral (2PAv) regions, by microsurgical procedures (Figueiredo and Neves, 2019). These sub-regions were then associated with 2PP or 3/4PP endoderm. CAM-explants derived from 2PAv mesenchyme and 3/4PP endoderm associations displayed normal thymus formation (n=3/3, Figures 4j-l). Conversely, only one in six CAM-explants presented thymus when 3/4PP endoderm was associated with 2PAd mesenchyme, revealing its inhibitory properties for thymus formation. This property seems restricted to thymus potential, as parathyroid glands develop in the presence of 2PAd mesenchyme (n=5/5, Table S2). Of notice, the 1PA mesenchyme also showed permissive properties to thymus formation. Tissue associations of 3/4PP endoderm with 1PA mesenchyme were able to form a thymus (n=5/6, Figure S2). Together, these results show that the local mesenchyme of the pharyngeal arches regulates the potential thymic outcome in distinct pouches.

PA mesenchymal signals that regulate PP thymic potential.

To unravel the mesenchyme-derived signals that modulate thymus formation, we performed an unbiased, in-depth transcriptome analysis of isolated mesenchymal tissues from distinct PAs at cE2.5: 3/4PA, corresponding to a microenvironment favouring thymus formation; and the dorsal region of 2PA (2Pad), which we demonstrated as having inhibitory properties to thymus development (Figure 5a). Total RNA was isolated from three biological replicate samples from the two regions and mRNA libraries were generated for paired-end illumina sequencing. High quality RNA-seq datasets were recovered for all samples, with an average of 7.7 million reads mapping uniquely to the *Gallus gallus* genome, corresponding to an average detection of ~15 400 genes (Supplementary Dataset 1). Of these, 532 transcripts were found to be

differentially expressed between 3/4PA and 2PAd with a log2FC >0.6 (adj pval <0.01) (Figures 5b-c, a complete list of genes in Supplementary Dataset 2).

The inBio Discover analysis of Top 5 Gene ontology (GO) – Bio.Process of the 317 upregulated genes in 3/4PA mesenchyme, revealed an enrichment in GO-terms related to vascular development processes (Figure 5d). Similar results were obtained for the 176 upregulated genes in 2PAd mesenchyme. Still, an enrichment in GO-terms related to epithelial to mesenchymal transition (EMT) processes was also identified for these transcripts (Figure 5d).

A detailed inspection of major signalling pathways (VEGF, Retinoid Acid, BMP, Wnt, Notch, EPH-Ephrin, FGF and Hedgehog) was also performed (Figure 5e and Table 2). We found a clear difference in gene enrichment for distinct signalling pathways when the two tissues were compared.

As expected, several transcripts for BMP ligands were up-regulated in the 3/4PA mesenchyme (Bleul and Boehm, 2005; Gordon et al., 2010; Jerome-majewska et al., 2002; Neves et al., 2012; Patel et al., 2006), when compared to 2PAd mesenchyme. Regarding Notch signalling, the observed enrichment of JAG1 expression in the 3/4PP endoderm confirms previous data from our lab (Figueiredo et al., 2016), suggesting an endogenous paracrine effect regulating 3/4PP specification, possibly via NOTCH1, whose expression is enriched in PP endoderm, when comparing with anterior Pharynx endoderm (Figure 2e).

Considering the number of genes found to be annotated to different signaling pathways, we find that the highest number in the 3/4PA mesenchyme is associated to the VEGF pathway followed by the Retinoic acid, BMP and Wnt pathways (in decreasing order).

In contrast, Wnt signalling seems to be the main up-regulated signaling pathway in 2PAd mesenchyme, suggesting its involvement in the inhibitory properties of this tissue (Figure 5e). The exception is WNT5A, which shows much higher expression in 3/4PA mesenchyme. In a comparable developmental process, it was shown that WNT5A secretion by dermal cells leads to autocrine FGF7 expression and consequent induction of FOXN1 expression in hair follicular cells (Hu et al., 2010). Our data also reveals FGF7 as the most enriched FGF-related transcript in 3/4PA mesenchyme, pointing to a similar WNT5A/FGF7/FOXN1 cascade in thymus induction at 3/4PP endoderm, probably mediated by fibroblast growth factor receptor R2-IIIb (Revest et al., 2001).

To search for other signals that may regulate epithelial-mesenchymal interactions during PP endoderm specification, we performed a similar approach exploring gene enrichment for distinct signalling pathways by comparing the 3/4PP and 2PP endoderm (Figure 5f, and Table 3). Notably, the most represented signalling pathways in 3/4PP and 2PP endoderm (Figure 5f) almost mirror the 3/4PA and 2PAd mesenchyme pathway profiles (Figure 5e). Again, transcripts

for Wnt signalling components are enriched in 2PP endoderm, in comparison to 3/4PP endoderm. Together, these results reinforce the hypothesis of the Wnt pathway acting as a silencer at this developmental stage, similar to what is observed in later stages of thymus formation (Swann et al., 2017). As detailed above, a strong correlation was established between up-regulated genes in 2PP endoderm and GO-terms of negative regulation of developmental processes (Figure 3b).

In contrast, VEGF and Retinoic Acid pathways show the highest transcript enrichment in 3/4PP and 3/4PA tissues, suggesting an essential role of these pathways during epithelial-mesenchymal interactions to promote thymus formation. The up-regulation of transcripts for RARB and other RA pathway components (Table 3), accompanied by strong up-regulation of HOX-gene expression (Figures 3c-d) in 3/4PP endoderm, clearly point to a critical role of the RA/Hox gene pathway in establishing the identity of this pharyngeal pouch.

A closer examination of secreted VEGF ligands shows a differential enrichment of VEGFA and VEGFD transcripts in the 3/4PP-3/4PA and 2PP-2PAd environments, respectively. This finding suggests a distinct activation of VEGF pathway to either promote or repress thymus formation. In agreement, VEGFA deletion from thymic epithelial cells disrupts organ blood vessel architecture (Mü et al., 2005).

Finally, specific ligand-receptor interactions of Ephrin signalling are suggested when analysing Ephrin related transcripts that are differentially expressed in 3/4PA – 3/4PP and 2PAd – 2PP environments (Tables 2 and 3). Ephrin signalling is known to participate in several thymus developmental scenarios [reviewed in (Muñoz et al., 2011)] and EFNB2 ligand was shown to be required for thymus migration during organogenesis (Foster et al., 2010). Herein, we identify transcript enrichment for EPHB1 in 3/4PP endoderm, suggesting Ephrin signalling activation by this receptor during 3/4PP endoderm specification.

Overall, our data provide a better understanding of the molecular processes underlying interactions between pharyngeal pouch endoderm and pharyngeal arch mesenchyme that precede thymus formation. This information shall help not only to explore the signals and cellular properties that regulate thymus specification in the embryo, but also to design improved organoid systems that recapitulate epithelial-mesenchymal interactions and lead to efficient ex vivo generation of thymic organs for regenerative purposes.

MATERIALS AND METHODS

Isolation of quail and chick embryonic tissues

Fertilised Japanese quail (*Coturnix coturnix japonica*) and chicken (Gallus gallus) eggs were incubated at 38 °C in a humidified incubator and embryos were dissected at specific times of development. Embryos were staged by microscopic examination according to Hamburger and Hamilton stages (HH, Hamburger and Hamilton, 1951) in the chick and to corresponding HH-stages in the quail. Isolation of 2PP and 3/4PP endoderm was performed at embryonic day 3 (E3, HH-stage 21) of quail embryos and at E2.5 (HH-stage 19-20) of chick embryos, as previously described (Figueiredo and Neves, 2019; Le Douarin and Jotereau, 1975; Neves et al., 2012). Briefly, pharyngeal tissues were obtained by treating the wall of the embryonic pharynx with a solution of pancreatin (8 mg/ml, Sigma) for 30–90 min on ice, which allowed separation of pure endoderm from the pharyngeal mesenchyme. Mesenchymal tissues of E2.5–E3 (HH-stages 18–19) chick embryos were dissociated from endodermal and ectodermal tissues by enzymatic digestion with pancreatin using the same procedure described above. Somatopleura tissues were obtained from the embryonic territories at the level of somites 19–24 (Figueiredo and Neves, 2019).

In vitro tissue culture assay

2PP and 3/4PP endoderm were isolated from E3 quail embryos and grown in association with mesenchymal tissues isolated from E2.5 chick embryos, as described (Figueiredo and Neves, 2019; Neves et al., 2012). Different sources of mesenchymal tissues were isolated: Somatopleura mesoderm; 3/4PA mesenchyme; 2PA mesenchyme; ventral territory of 2PA mesenchyme (2PAv); and dorsal territory of 2PA mesenchyme (2PAd). In brief, 2–3 endodermal explants (2PP or 3/4PP endoderm) were combined with 2–3 mesenchymal explants on Nucleopore membrane filters (Millipore) supported by fine meshed metal grids (Goodfellows). The grids were then placed into culture dishes and partly immersed in RPMI-1640 (Sigma) supplemented with 10% FBS (Invitrogen) and 1X Pen/Strep (Invitrogen). The heterospecific associated tissues were cultured for 48 h at 37 °C in a humidified incubator containing 5% CO_2. Following the incubation period, cultured tissues were either used for RNA isolation or grafted on the chorioallantoic membrane (CAM) of E8-chick embryos. Grafted tissues were allowed to further develop in ovo for 10 days in a humidified incubator at 38 °C, as described (Le Douarin and Jotereau, 1975; Neves et al., 2012).

Immunohistochemistry

CAM-derived explants were fixed overnight in 4% paraformaldehyde/PBS at 4°C. Samples were then processed for immunohistochemistry, as described (Figueiredo et al., 2016).

Paraffin sections of explants developed *in ovo* for 10 days were analysed by haematoxylin-eosin staining (H&E) to determine the number, size and morphology of thymic lobes and parathyroid glands formed. Sections of CAM-explants were further treated for immunocytochemistry with the QCPN antibody (for labelling of quail cells), CD3 antibody (Dako M725429-2, for labelling T-lymphoid cells) and anti-pan [Lu-5] Cytokeratin antibody (Pan CK) (Abcam; for labelling epithelial cells), as described (Figueiredo and Neves, 2018; Neves et al., 2012) .

Flow Cytometry

Thymi were isolated from Chicken embryos at specific time points: E11, E12, E13, E15, E17 and E18. Thymocytes suspensions were prepared by mechanically disrupting the thymus by gently pressing the tissue through a fine nylon mesh (pore size 70 μ m) to obtain a single cell suspension. The suspension was then purified by Ficoll density gradient separation (Ficoll- Paque PLUS GE Healthcare Life Sciences), to remove dead cells and red blood cells. Cells were stained using a panel of mouse anti-chicken monoclonal antibodies from Southern Biotech: anti-CD4 FITC (clone CT-4), anti-CD8 FITC (clone CT-8), anti-CD8 PE (clone CT-8) and anti-CD3 PE (clone CT-3) according to manufacturer's instructions. Cells were analyzed on LSR Fortessa cytometer (BD) and data analyzed using FlowJo software (TreeStar).

Microscopy

H&E and immunohistochemistry images were collected using Software Leica Firewire and Leica DM2500 microscope with Leica DFC420 camera.

RNA library preparation

Total RNA from the samples was extracted using a combination of TRIzol reagent (Invitrogen) and RNeasy Mini Kit (QIAGEN) according to the manufacturer's instructions (Figueiredo et al., 2016). RNA samples were obtained from freshly isolated embryonic tissues of quail endoderm at E3 and chicken mesenchyme at E2.5. The isolated endoderm tissues were 2PP endoderm, 3/4PP endoderm and central pharynx region (Pharynx). The isolated mesenchyme tissues were 3/4PA mesenchyme and dorsal territory of 2PA mesenchyme (2PAd). Three replicates of 15-20

explants per sample were generated for each condition. Total RNA samples were validated for concentration and integrity (RIN ≥ 7) and 1 µg of total RNA was used to prepare libraries with the Stranded mRNA Library Preparation Kit according to manufacturer's instructions. Libraries were sequenced on an Illumina Novaseq platform with paired end 150bp reads (acquired as a service to STAB Vida), with an average yield of 25M reads per sample (R1+R2). The raw RNA-Seq datasets are available through the European Nucleotide Archive under the study accession number PRJEB51508 (Gallus gallus dataset) and PRJEB51507 (C. coturnix dataset).

RNA-Seq data analysis

Following quality assessment using FastQC version 0.11.5 (https://www.bioinformatics.babraham.ac.uk/projects/fastqc/), Cutadapt was used to remove sequencing adaptors and trim the first 10 nucleotides (Martin, 2011). The trimmed data was then filtered using in-house developed Perl script in order to remove reads with unknown nucleotides, homopolymers with length ≥50 nt or an average Phred score <30 (Amaral et al., 2014). Remaining reads, corresponding on average to 80% of the raw data, were aligned to the Ensemble genome references Coturnix_japonica_2.0 (GCA_001577835.1) or GRCg6a (GCA_000002315.5) for quail or chicken libraries, respectively. Alignment was performed using STAR version 2.5.0 with the following options: –outFilterType BySJout –alignSJoverhangMin 8 –alignSJDBoverhangMin 5 –alignIntronMax 100000 –outSAMtype BAM SortedByCoordinate –twopassMode Basic –outFilterScoreMinOverLread 0 –outFilterMatchNminOverLread 0 –outFilterMatchNmin 0 –outFilterMultimapNmax 1 –limitBAMsortRAM 10000000000 –quantMode GeneCounts (Dobin et al., 2013). Gene counts were determined using the htseq-count function from HTseq (version 0.9.1) (Anders et al., 2015) in union mode and discarding low quality score alignments (–a 10), using the Ensembl Coturnix_japonica_2.0 or GRCg6a genome annotations. On average, 67% and 77% of the filtered reads from quail and chicken samples mapped to a single genomic location, corresponding to ∼14 500 and ∼15 400 detected genes, respectively. Supplementary Dataset 1 presents the summary information of the RNA-seq datasets.

Clustering of normalized gene counts and Principal Component Analysis (PCA) for exploratory data analysis were performed with the pheatmap R package using the euclidean distance matrix computation of the dist function, and the ggfortify:plotPCA function, respectively.

Differential Expression Analysis (DEA) for RNA-Seq gene counts was performed with the limma Bioconductor package using the voom method to convert the read-counts to log2-cpm, with associated weights, for linear modeling (Law et al., 2014; Ritchie et al., 2015). Differential gene

expression analysis was performed by making all possible comparisons between the three C. japonica experimental conditions or by comparing the two G. gallus experimental conditions, using all available replicate data. Genes showing up or down-regulation with an adjusted *p value* <0.01 and a log2 fold change (log2FC) of |log2FC|>0.6 were considered differentially expressed.

GO analysis to elucidate potential biological processes associated to up-regulated genes in was performed using inBio Discover (Li et al., 2017)

Heatmaps for differentially expressed genes were generated using the pheatmap function from the R pheatmap package with the ward.D or complete clustering method, for all genes or only transcription factors, respectively.

Functional Enrichment Analysis

Functional annotations were downloaded from Ensembl Genes 105 for the quail (Coturnix_japonica_2.0) and chicken (GRCg6a) genes using the integrated Biomart interface. Functional enrichment of differentially expressed genes was performed with the GOfuncR package version 1.14.0 using all the detected genes in our dataset as background and the core function goenrich with default parameters (hypergeometric test, 1000 randomizations), considering as significant as FDR < 0.01.

ACKNOWLEDGMENTS

The authors are grateful to Leonor Parreira and Georg Hollander for helping raise this project from the ground and to Edgar Gomes, Rita Zilhão and António Cidadão for useful discussions. We are also thankful to Solveig Thorsteinsdottir for reagents and Interaves Portugal for contributing with quail fertilised eggs. This work was supported by Fundação para a Ciência e para a Tecnologia (FCT), project PTDC/SAU-BID/115264/2009 and Leonor Magalhães received two research grants from GAPIC. Work in MGC's lab is supported by FCT – Fundação para a Ciência e Tecnologia, Portugal through grants UIDB/04046/2020 and UIDP/04046/2020 Centre grants from FCT (to BioISI).

CONFLICTS OF INTEREST

The authors declare no conflict of interests.

DATA AVAILABILITY

The 30 raw fastq files of the RNA-seq data generated for this study have been submitted to the European Nucleotide Archive under the umbrella project "Thymus inception" (PRJEB51509), with individual study accession numbers PRJEB51507 (quail dataset) and PRJEB51508 (chicken dataset).

AUTHOR CONTRIBUTIONS

HN contributed to the conceptualization, design of experiments, experiment execution and analysis of results. IA and LM carried out the experiments. MGC contributed to the experimental design of the transcriptome profiling and performed the RNA-seq data analysis. VP contributed with technical support. DH and MGC contributed to the analysis of results. HN and DH wrote the manuscript.

REFERENCES

Ainsworth, S. J., Stanley, R. L. and Evans, D. J. R. (2010). Developmental stages of the Japanese quail. *J. Anat.* **216**,.

Amaral, A. J., Brito, F. F., Chobanyan, T., Yoshikawa, S., Yokokura, T., Van Vactor, D. and Gama-Carvalho, M. (2014). Quality assessment and control of tissue specific RNA-seq libraries of Drosophila transgenic RNAi models. *Front. Genet.* **5**,.

Anders, S., Pyl, P. T. and Huber, W. (2015). HTSeq--a Python framework to work with high-throughput sequencing data. *Bioinformatics* **31**, 166–169.

Bautista, J. L., Cramer, N. T., Miller, C. N., Chavez, J., Berrios, D. I., Byrnes, L. E., Germino, J., Ntranos, V., Sneddon, J. B., Burt, T. D., et al. (2021). Single-cell transcriptional profiling of human thymic stroma uncovers novel cellular heterogeneity in the thymic medulla. *Nat. Commun.* **12**, 1096.

Bleul, C. C. and Boehm, T. (2005). BMP signaling is required for normal thymus development. *J. Immunol.* **175**, 5213–21.

Dobin, A., Davis, C. A., Schlesinger, F., Drenkow, J., Zaleski, C., Jha, S., Batut, P., Chaisson, M. and Gingeras, T. R. (2013). STAR: ultrafast universal RNA-seq aligner. *Bioinformatics* **29**, 15–21.

Enkhmandakh, B. and Bayarsaihan, D. (2015). Genome-wide Chromatin Mapping Defines AP2α in the Etiology of Craniofacial Disorders. *Cleft Palate-Craniofacial J.* **52**, 135–142.

Figueiredo, M. and Neves, H. (2018). Two-step Approach to Explore Early-and Late-stages of Organ Formation in the Avian Model: The Thymus and Parathyroid Glands Organogenesis Paradigm Video Link. *J. Vis. Exp* **5711437915**,.

Figueiredo, M. and Neves, H. (2019). Isolation of Embryonic Tissues and Formation of Quail-Chicken Chimeric Organs Using The Thymus Example. *J. Vis. Exp.* e58965.

Figueiredo, M., Silva, J. C., Santos, A. S., Proa, V., Alcobia, I., Zilhão, R., Cidadão, A. and Neves, H. (2016). Notch and Hedgehog in the thymus/parathyroid common primordium: Crosstalk in organ formation. *Dev. Biol.* **418**, 268–282.

Figueiredo, M., Zilhão, R. and Neves, H. (2020). Thymus Inception: Molecular Network in the Early Stages of Thymus Organogenesis. *Int. J. Mol. Sci.* **21**, 5765.

Foster, K. E., Gordon, J., Cardenas, K., Veiga-Fernandes, H., Makinen, T., Grigorieva, E., Wilkinson, D. G., Clare Blackburng, C., Richie, E., Manley, N. R., et al. (2010). EphB-ephrin-B2 interactions are required for thymus migration during organogenesis. *Proc. Natl. Acad. Sci. U. S. A.* **107**, 13414–13419.

Gordon, J., A, B, Patel, S. R., Mishina, Y. and Manley, N. R. (2010). Evidence for an early role for BMP4 signaling in thymus and parathyroid morphogenesis. *Dev. Biol.* **339**, 141–154.

Hu, B., Lefort, K., Qiu, W., Nguyen, B. C., Rajaram, R. D., Castillo, E., He, F., Chen, Y., Angel, P., Brisken, C., et al. (2010). Control of hair follicle cell fate by underlying mesenchyme through a CSL-Wnt5a-FoxN1 regulatory axis. *Genes Dev.* **24**, 1519–1532.

Jerome-majewska, L. A., Papaioannou, V. E., Ohnemus, S. and Boehm, T. (2002). Aortic arch and pharyngeal phenotype in the absence of BMP-dependent neural crest in the mouse. **119**, 127–135.

Kamitani-Kawamoto, A., Hamada, M., Moriguchi, T., Miyai, M., Saji, F., Hatamura, I., Nishikawa, K., Takayanagi, H., Hitoshi, S., Ikenaka, K., et al. (2011). MafB interacts with Gcm2 and regulates parathyroid hormone expression and parathyroid development. *J. Bone Miner. Res.* **26**, 2463–2472.

Khatri, S. B. and Groves, A. K. (2013). Expression of the Foxi2 and Foxi3 transcription factors during development of chicken sensory placodes and pharyngeal arches. *Gene Expr. Patterns* **13**, 38–42.

Law, C. W., Chen, Y., Shi, W. and Smyth, G. K. (2014). voom: precision weights unlock linear model analysis tools for RNA-seq read counts. *Genome Biol.* **15**, R29.

Le Douarin, N. M. and Jotereau, F. V (1975). Tracing of cells of the avian thymus through embryonic life in interspecific chimeras. *J. Exp. Med.* **142**, 17–40.

Le Lièvre, C. S. and Le Douarin, N. M. (1975). Mesenchymal derivatives of the neural crest: analysis of chimaeric quail and chick embryos. *J. Embryol. Exp. Morphol.* **34**, 125–154.

Li, X., Oghi, K. a, Zhang, J., Krones, A., Bush, K. T., Glass, C. K., Nigam, S. K., Aggarwal, A. K., Maas, R., Rose, D. W., et al. (2003). Eya protein phosphatase activity regulates Six1-Dach-Eya transcriptional effects in mammalian organogenesis. *Nature* **426**, 247–254.

Li, T., Wernersson, R., Hansen, R. B., Horn, H., Mercer, J., Slodkowicz, G., Workman, C. T., Rigina, O., Rapacki, K., Stærfeldt, H. H., et al. (2017). A scored human protein–protein interaction network to catalyze genomic interpretation. *Nat. Methods* **14**, 61–64.

Magaletta, M. E., Lobo, M., Kernfeld, E. M., Aliee, H., Huey, J. D., Parsons, T. J., Theis, F. J. and Maehr, R. (2022). Integration of single-cell transcriptomes and chromatin landscapes reveals regulatory programs driving pharyngeal organ development. *Nat. Commun.* **13**, 457.

Martin, M. (2011). Cutadapt removes adapter sequences from high-throughput sequencing reads. *EMBnet.journal* **17**, 10.

Mü, S. M., Terszowski, G., Blum, C., Haller, C., Anquez, V., Kuschert, S., Carmeliet, P., Augustin, H. G. and Rodewald, H.-R. (2005). *Gene targeting of VEGF-A in thymus epithelium disrupts thymus blood vessel architecture*.

Muñoz, J. J., Cejalvo, T., Alonso-Colmenar, L. M., Alfaro, D., Garcia-Ceca, J. and Zapata, A. (2011). Eph/ephrin-mediated interactions in the thymus. *Neuroimmunomodulation* **18**, 271–280.

Neves, H., Dupin, E., Parreira, L. and Le Douarin, N. M. (2012). Modulation of Bmp4 signalling in the epithelial-mesenchymal interactions that take place in early thymus and parathyroid development in avian embryos. *Dev. Biol.* **361**, 208–219.

Park, J.-E., Botting, R. A., Domínguez Conde, C., Popescu, D.-M., Lavaert, M., Kunz, D. J., Goh, I., Stephenson, E., Ragazzini, R., Tuck, E., et al. (2020). A cell atlas of human thymic development defines T cell repertoire formation. *Science (80-.).* **367**,.

Patel, S. R., Gordon, J., Mahbub, F., Blackburn, C. C. and Manley, N. R. (2006). Bmp4 and Noggin expression during early thymus and parathyroid organogenesis. *Gene Expr. patterns GEP* **6**, 794–799.

Revest, J. M., Suniara, R. K., Kerr, K., Owen, J. J. and Dickson, C. (2001). Development of the thymus requires signaling through the fibroblast growth factor receptor R2-IIIb. *J. Immunol.* **167**, 1954–1961.

Reynolds, K., Kumari, P., Sepulveda Rincon, L., Gu, R., Ji, Y., Kumar, S. and Zhou, C. J. (2019). Wnt signaling in orofacial clefts: crosstalk, pathogenesis and models. *Dis. Model. Mech.* **12**,.

Reynolds, K., Zhang, S., Sun, B., Garland, M. A., Ji, Y. and Zhou, C. J. (2020). Genetics and signaling mechanisms of orofacial clefts. *Birth Defects Res.* **112**, 1588–1634.

Ritchie, M. E., Phipson, B., Wu, D., Hu, Y., Law, C. W., Shi, W. and Smyth, G. K. (2015). limma powers differential expression analyses for RNA-sequencing and microarray studies. *Nucleic Acids Res.* **43**, e47–e47.

Rizzoti, K. and Lovell-Badge, R. (2007). SOX3 activity during pharyngeal segmentation is required for craniofacial morphogenesis. *Development* **134**, 3437–3448.

Swann, J. B., Happe, C. and Boehm, T. (2017). Elevated levels of Wnt signaling disrupt thymus morphogenesis and function. *Sci. Rep.* **7**,.

LEGENDS TO FIGURES

FIGURE 1 | Thymus formation in CAM-derived explants of PP endoderm and somatopleura mesoderm associations. Serial sections of thymi stained with H&E (a and d), and immunodetected with QCPN (quail cells) (b and e) and CD3 (T-cells) (c and f) antibodies. Top panel (a-c) - Thymus derived from associations of quail 3PP endoderm with chicken SM. Bottom panel (d-e) - Thymus derived from associations of quail 2PP endoderm with chicken SM. Arrowheads point immunostaining positive cells for QCPN (quail thymic epithelium) and for CD3 (chicken T-cells differentiated in the thymus). CAM, chorioallantoic membrane; E, embryonic day; PA, Pharyngeal Arch; PP, Pharyngeal Pouch; SM, somatopleura mesoderm. Scale bars, 100μm.

FIGURE 2 | Transcriptional profiles of pharyngeal endoderm tissues. a) Schematic representation of distinct endoderm tissues isolated from the embryonic pharyngeal region at qE3. b) Heatmap showing differentially expressed genes in the pharynx, 3/4PP and 2PP endoderm (fold change >0.6 and <−0.6, and *P*-value <0.01). Volcano plots depict differentially expressed transcripts of 3/4PP (c) and 2PP (d) comparing with the pharynx. Red dots highlight transcripts passing the log2FC and adj pvalue cut-offs and blue dots highlights trasncripts with adj pval <0.01. e) Schematic representation of the genetic profile of distinct PP progenitors considering the enrichment of up-regulated transcription factors and regulators when comparing PPs with the pharynx. PP, Pharyngeal Pouch.

FIGURE 3 | Differential gene expression analyses reveal discrete transcriptomic signature of 2PP and 3/4PP endoderm. a) Heatmap showing differentially expressed genes in 3/4PP and 2PP endoderm (fold change >0.6 and <−0.6, and *P*-value <0.01). b) Bar plot depicting inBio Discover analysis of Top 5 Gene ontology (GO) – Bio.Process for 518 genes differentially expressed in 3/4PP and 2PP endoderm. c) Volcano plot depict differentially expressed transcripts of 3/4PP

endoderm comparing with the 2PP endoderm. Red dots highlight transcripts passing the log2FC and adj pvalue cut-offs and blue dots highlights trasncripts with adj pval <0.01. a) Heatmap showing the selected transcription factors and regulators differentially expressed in 3/4PP and 2PP endoderm. ASF, Anatomical structure formation; PP, Pharyngeal Pouch.

FIGURE 4 | Thymus formation in CAM-derived explants of PP endoderm and mesenchyme associations. Serial sections of thymi stained with H&E (a, d, g and j), and immunodetected with QCPN (quail cells) (b, e, h and k) and CD3 (T-cells) (c, f, i and l) antibodies. First panel (a-c) - thymus derived from associations of quail 2PP endoderm with chicken 3/4PA mesenchyme. Second panel (d-f) - thymus derived from associations of quail 3/4PP endoderm with chicken 3/4PA mesenchyme. Third panel (g-i) - thymus derived from associations of quail 3/4PP endoderm with chicken 2PA mesenchyme. Fourth panel (j-l) - thymus derived from associations of quail 3/4PP endoderm with chicken ventral territory of 2PA mesenchyme. Arrowheads point immunostaining positive cells for QCPN (quail thymic epithelium) and for CD3 (chicken T-cells differentiated in the thymus). CAM, chorioallantoic membrane; E, embryonic day; PA, Pharyngeal Arch; PP, Pharyngeal Pouch. Scale bars, 100μm.

FIGURE 5 | Transcriptional profiles of pharyngeal mesenchyme tissues. a) Schematic representation of distinct mesenchyme tissues isolated from the embryonic pharyngeal region at qE3. b) Heatmap showing differentially expressed genes in the 2PAd and 3/4PA (fold change >0.6 and <−0.6, and *P*-value <0.01). c) Volcano plot depict differentially expressed transcripts of 3/4PA comparing with 2PAd. Red dots highlight transcripts passing the log2FC and adj pvalue cut-offs and blue dots highlights trasncripts with adj pval <0.01. d) Bar plot depicting inBio Discover analysis of Top 5 Gene ontology (GO) – Bio.Process for 317 genes differentially expressed in 3/4PA mesenchyme versus 2PAd mesenchyme.
e) Treemap depict up-regulated transcripts of major signalling pathways, VEGF, Retinoid Acid, BMP, Wnt, Notch, EPH-Ephrin, FGF and Hedgehog in 3/4PA and 2PAd. f) Treemap depict up-regulated transcripts of major signalling pathways, VEGF, Retinoid Acid, BMP, Wnt, Notch, EPH-Ephrin, FGF and Hedgehog in 3/4PP and 2PP. CSRSP Cell surface receptor signaling pathway; ETM, epithelial to mesenchymal transition; PA, Pharyngeal Arch; PP, Pharyngeal Pouch.

Figure 1.

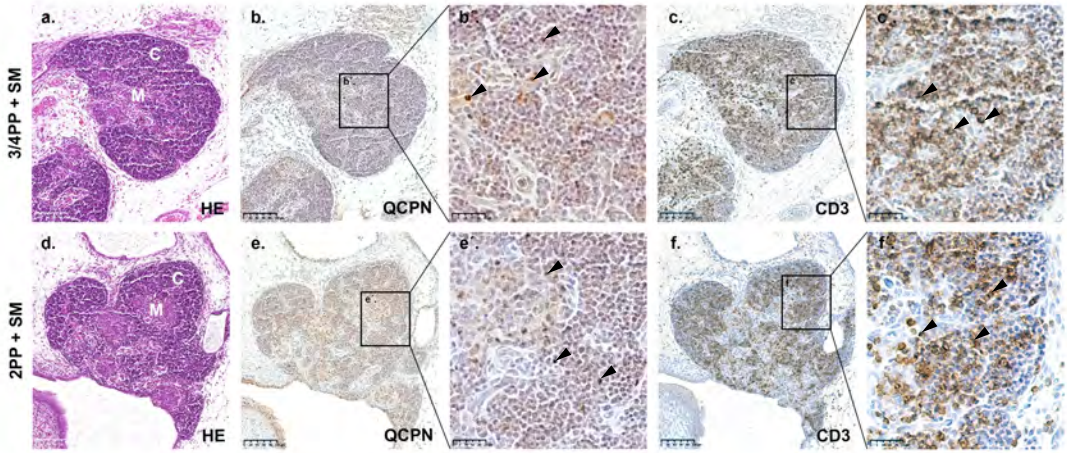

Figure 2.

a.

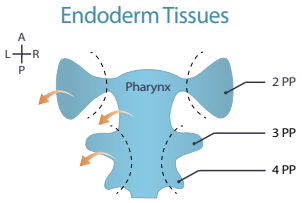

b.

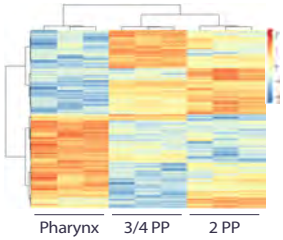

c.

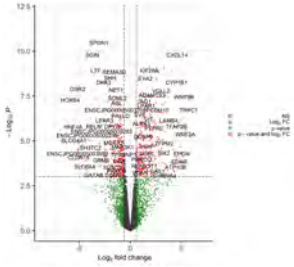

d.

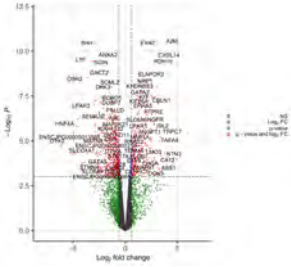

e.

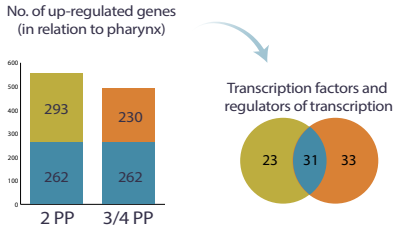

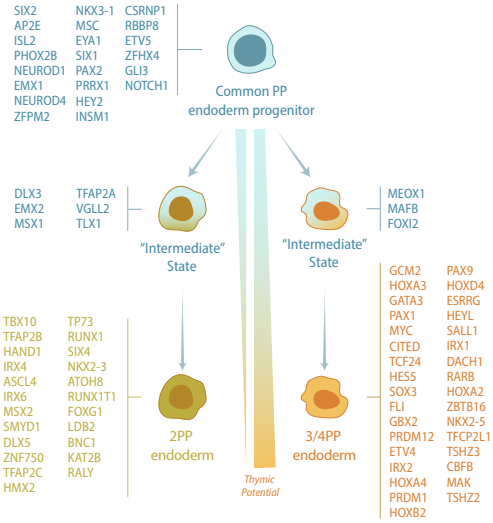

Figure 3.

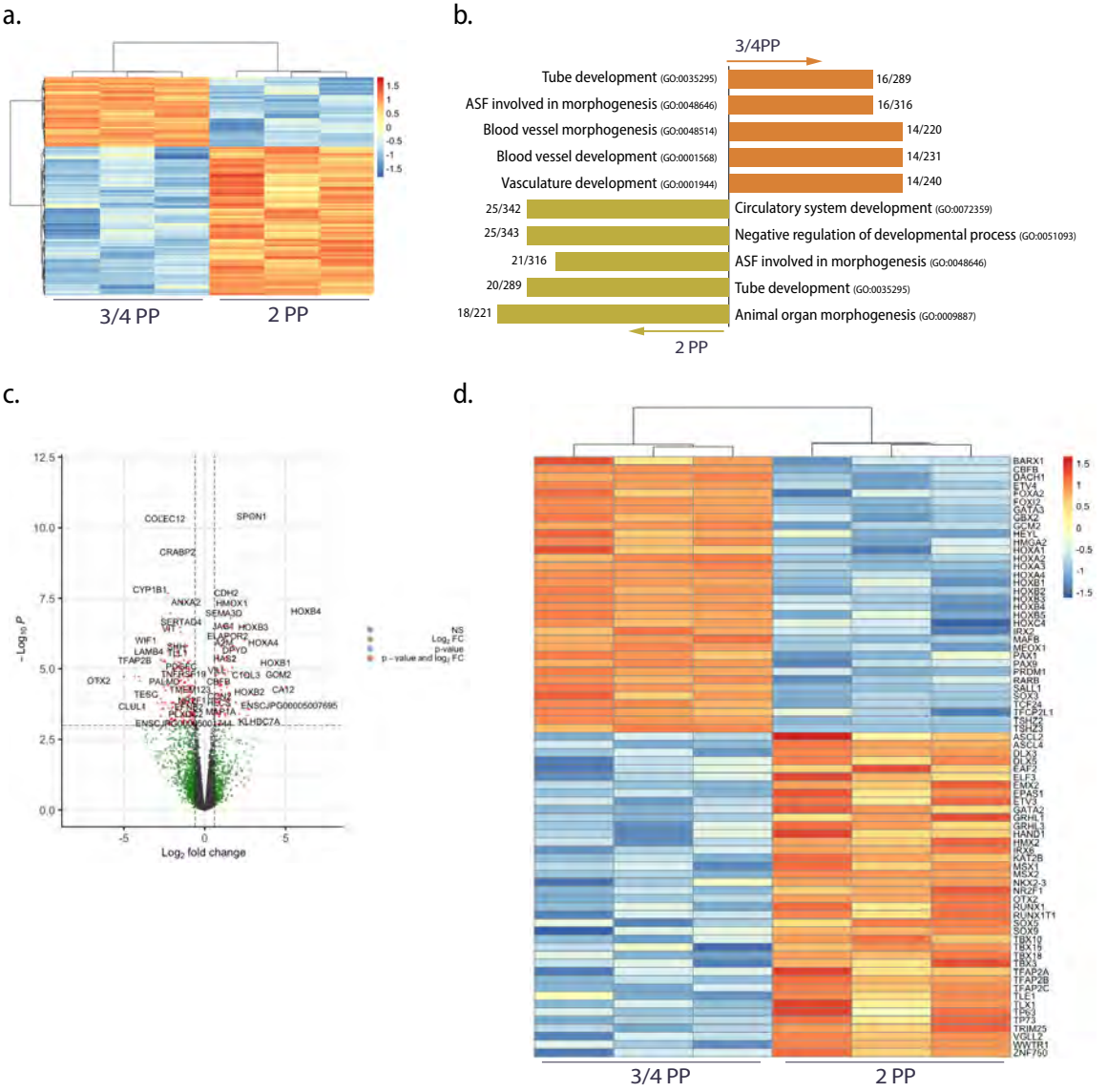
a.
1.5
1
0.5
0
-0.5
-1
-1.5
3/4 PP
2 PP
b.
3/4PP
Tube development (GO:0035295)
16/289
ASF involved in morphogenesis (GO:0048646)
16/316
Blood vessel morphogenesis (GO:0048514)
14/220
Blood vessel development (GO:0001568)
14/231
Vasculature development (GO:0001944)
14/240
25/342
Circulatory system development (GO:0072359)
25/343
Negative regulation of developmental process (GO:0051093)
21/316
ASF involved in morphogenesis (GO:0048646)
20/289
Tube development (GO:0035295)
18/221
Animal organ morphogenesis (GO:0009887)
2 PP
c.
12.5
10.0
7.5
5.0
2.5
0.0
-5
0
5
$-\log_{10} P$
$\log_2$ fold change
COLEC12
SPON1
CRABP2
CYP1B1
ANXA2
CDH2
HMOX1
SEMA3D
HOXB4
SERTAD4
VIT
JAG1
HOXB3
ELAPOR2
WIF1
LAMB4
TFAP2B
HOXA4
DPYD
HAS2
HOXB1
OTX2
PALMD
CBFB
CTOL3
GCM2
TESC
HOXB2
CA12
CLUL1
ENSCJPG00005007695
KLHDC7A
NS
$\log_2$ FC
p-value
p-value and $\log_2$ FC
d.
1.5
1
0.5
0
-0.5
-1
-1.5
3/4 PP
2 PP

Figure 4.

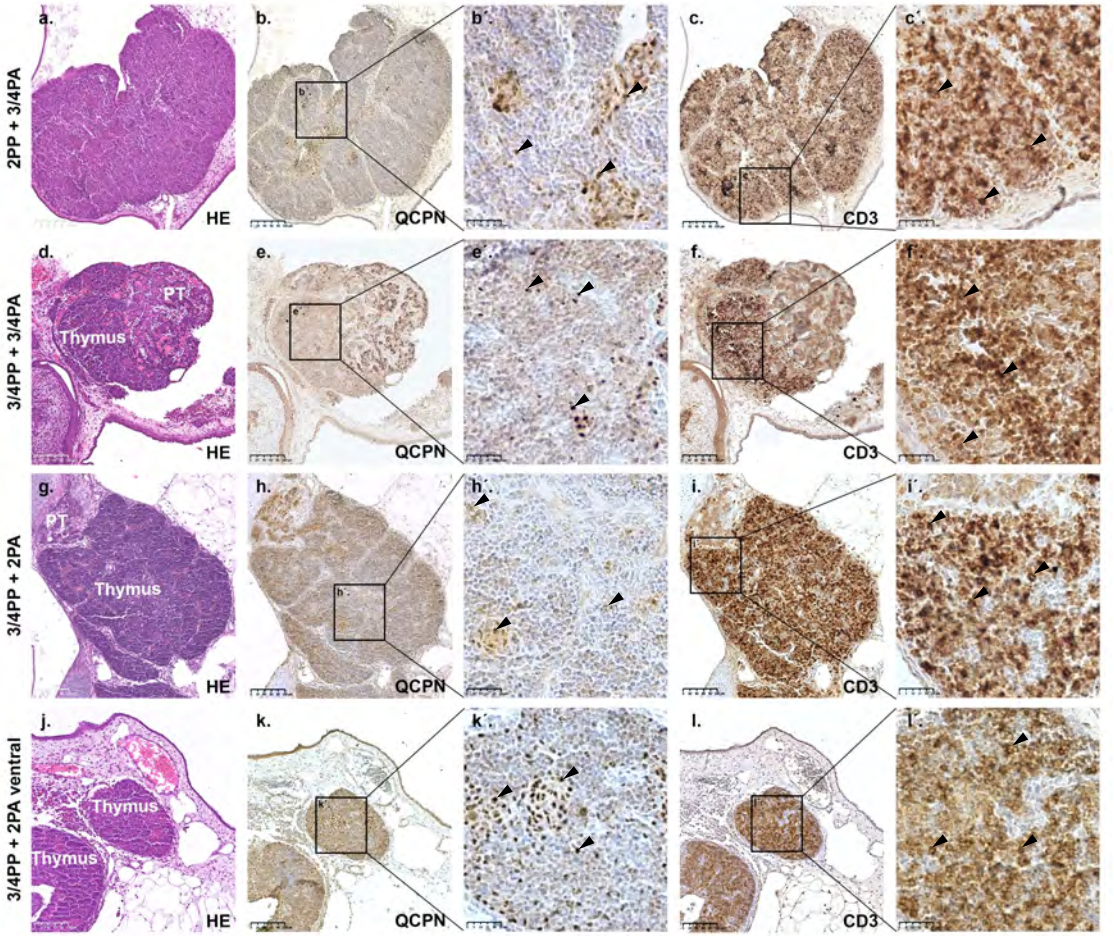
2PP + 3/4PA
3/4PP + 3/4PA
3/4PP + 2PA
3/4PP + 2PA ventral
a.
b.
b´.
c.
c´.
d.
e.
e´.
f.
f´.
g.
h.
h´.
i.
i´.
j.
k.
k´.
l.
l´.
PT
Thymus
Thymus
Thymus
HE
QCPN
CD3

Figure 5.

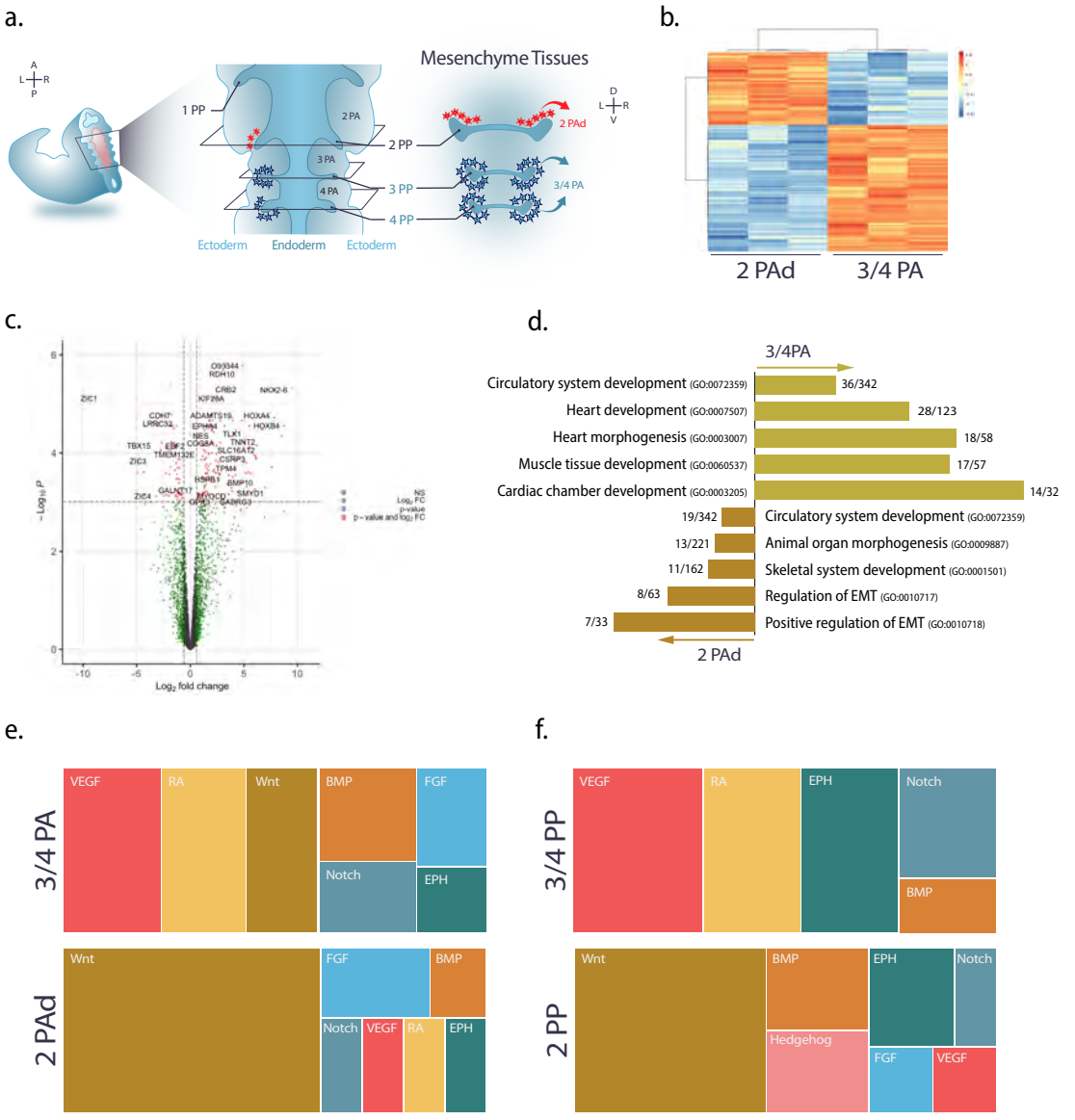
a.
Mesenchyme Tissues
1 PP
2 PA
3 PA
4 PA
2 PP
3 PP
4 PP
2 PAd
3/4 PA
Ectoderm
Endoderm
Ectoderm
b.
2 PAd
3/4 PA
c.
Log2 fold change
d.
3/4PA
Circulatory system development (GO:0072359) 36/342
Heart development (GO:0007507) 28/123
Heart morphogenesis (GO:0003007) 18/58
Muscle tissue development (GO:0060537) 17/57
Cardiac chamber development (GO:0003205) 14/32
19/342 Circulatory system development (GO:0072359)
13/221 Animal organ morphogenesis (GO:0009887)
11/162 Skeletal system development (GO:0001501)
8/63 Regulation of EMT (GO:0010717)
7/33 Positive regulation of EMT (GO:0010718)
2 PAd
e.
3/4 PA
VEGF
RA
Wnt
BMP
FGF
Notch
EPH
2 PAd
Wnt
FGF
BMP
Notch
VEGF
RA
EPH
f.
3/4 PP
VEGF
RA
EPH
Notch
BMP
2 PP
Wnt
BMP
EPH
Notch
Hedgehog
FGF
VEGF

Table 1. **Chimeric thymus in CAM-explants.**

Heterospecific association of tissues	2PP endoderm	3/4PP endoderm
Somatopleura mesoderm	6/6	5/5
3/4 PA mesenchyme	3/3	3/3
2 PA mesenchyme	ND	2/3
2 PA mesenchyme - Ventral territory	ND	3/3
2 PA mesenchyme - Dorsal territory	ND	1/5

Number of samples with thymus per total number of samples. ND, Not Done.

Table 2. **Genes of main signalling pathways differentially expressed in PA mesenchyme.**

	3/4PA mesenchyme		2PAd mesenchyme	
Signaling by VEGF (R-HSA-194138)	VEGFA	Vascular endothelial growth factor A	VEGFD	Vascular endothelial growth factor D
	KDR	Vascular endothelial growth factor receptor 2		
	PAK1	Serine/threonine-protein kinase PAK 1		
	CYFIP2	Cytoplasmic FMR1-interacting protein 2		
	HSPB1	Heat shock protein beta-1		
	MAPK11	Mitogen-activated protein kinase 11		
	MAPK12	Mitogen-activated protein kinase 12		
Signaling by Retinoic Ac. (R-HSA-5362517)	RARA	Retinoic acid receptor alpha	CYP26C1	Cytochrome P450 26C1
	CRABP1	Cellular retinoic acid-binding protein 1		
	ALDH1A2	Retinal dehydrogenase 2		
	DHRS3	Short-chain dehydrogenase/reductase 3		
	RDH10	Retinol dehydrogenase 10		
	CYP26A1	Cytochrome P450 26A1		
BMP signaling pathway (GO:0030509)	BMP2	Bone morphogenetic protein 2	CHRDL1	Chordin-like protein 1
	BMP4	Bone morphogenetic protein 4		
	BMP6	Bone morphogenetic protein 6		
	BMP7	Bone morphogenetic protein 7		
	BMP10	Bone morphogenetic protein 10		
	GDF6	Growth/differentiation factor 6		
Wnt signaling pathway (GO:0016055)	WNT2	Protein Wnt-2	WIF1	Wnt inhibitory factor 1
	WNT2B	Protein Wnt-2b	SFRP1	Secreted frizzled-related protein 1
	WNT5A	Protein Wnt-5a	APCDD1	Protein APCDD1
	FZD8	Frizzled-8	AXIN2	Axin-2
	SFRP2	Secreted frizzled-related protein 2	DAB2	Disabled homolog 2
	DKK3	Dickkopf-related protein 3	NKD1	Protein naked cuticle homolog 1
	CTNND2	Catenin delta-2	TLE1	Transducin-like enhancer protein 1
			LGR4	Leucine-rich repeat-containing G-protein coupled receptor 4
			DIXDC1	Dixin
			CPZ	Carboxypeptidase Z
			LEF1	Lymphoid enhancer-binding factor 1
Notch signaling pathway (GO:0007219)	HES5	Transcription factor HES-5	SNAI2	Zinc finger protein SNAI2
	HOXD3	Homeobox protein Hox-D3		
	NEURL1B	E3 ubiquitin-protein ligase NEURL1B		
Ephrin signaling (R-HSA-3928664)	EPHA4	Ephrin type-A receptor 4	EFNB1	Ephrin-B1
	PAK1	Serine/threonine-protein kinase PAK 1		
Signaling by FGFR (R-HSA-190236)	FGF7	Fibroblast growth factor 7	FGF19	Fibroblast growth factor 19
	FGFRL1	Fibroblast growth factor receptor-like 1	FLRT3	Leucine-rich repeat transmembrane protein FLRT3
	SPRY2	Protein sprouty homolog 2		
Hedgehog Signaling Pathway (WP4249)				

Table 3. **Genes of main signalling pathways differentially expressed in PP endoderm.**

	3/4PP endoderm		2PP endoderm	
Signaling by VEGF (R-HSA-194138)	VEGFA	Vascular endothelial growth factor A	VEGFD	Vascular endothelial growth factor D
	NRP1	Neuropilin-1	PIK3R1	Phosphatidylinositol 3-kinase regulatory subunit alpha
	PIK3CB	Phosphatidylinositol 4,5-bisphosphate 3-kinase catalytic subunit beta isoform		
	PTK2	Focal adhesion kinase 1		
Signaling by Retinoic Ac. (R-HSA-5362517)	RARB	Retinoic acid receptor beta		
	CRABP1	Cellular retinoic acid-binding protein 1		
	RDH10	Retinol dehydrogenase 10		
BMP signaling pathway (GO:0030509)	CHRDL1	Chordin-like protein 1	GREM2	Gremlin-2
			GDF6	Growth/differentiation factor 6
			SOSTDC1	Sclerostin domain-containing protein 1
			TGFBR3	Transforming growth factor beta receptor type 3
Wnt signaling pathway (GO:0016055)			WNT2B	Protein Wnt-2b
			WNT3A	Protein Wnt-3a
			WNT6	Protein Wnt-6
			WNT7B	Protein Wnt-7b
			WNT7A	Protein Wnt-7a
			WNT9B	Protein Wnt-9b
			FZD10	Frizzled-10
			WIF1	Wnt inhibitory factor 1
			AXIN2	Axin-2
			APCDD1	Protein APCDD1
			DAB2	Disabled homolog 2
			LEF1	Lymphoid enhancer-binding factor 1
			RNF43	E3 ubiquitin-protein ligase RNF43
			KREMEN1	Kremen protein 1
			TRABD2A	Metalloprotease TIKI1
			NXN	Nucleoredoxin
			ROR1	Inactive tyrosine-protein kinase transmembrane receptor ROR1
			TLE1	Transducin-like enhancer protein 1
Notch signaling pathway (GO:0007219)	JAG1	Protein jagged-1	TP63	Tumor protein 63
	HEYL	Hairy/enhancer-of-split related with YRPW motif-like protein	SNAI2	Zinc finger protein SNAI2
			KAT2B	Histone acetyltransferase KAT2B
Ephrin signaling (R-HSA-3928664)	EPHB1	Ephrin type-B receptor 1	EFNB2	Ephrin-B2
	DNM1	Dynamin-1	EPHA1	Ephrin type-A receptor 1
	PTK2	Focal adhesion kinase 1	NGEF	Ephexin-1
			KALRN	Kalirin
Signaling by FGFR (R-HSA-190236)			ANOS1	Anosmin-1
			PIK3R1	Phosphatidylinositol 3-kinase regulatory subunit alpha
Hedgehog Signaling Pathway (WP4249)			SHH	Sonic hedgehog protein
			PTCH1	Protein patched homolog 1
			PTCH2	Protein patched homolog 2
			HHIP	Hedgehog-interacting protein
			LRP2	Low-density lipoprotein receptor-related protein 2